AN IMPROVED MODEL FOR FULL WAVE ANALYSIS OF MULTILAYERED FREQUENCY SELECTIVE SURFACE WITH GRIDDED SQUARE ELEMENT

A. Qing

Department of Electrical Engineering
University of Kassel
D-34109, Kassel, Germany

C. K. Lee

School of Electrical and Electronic Engineering
Nanyang Technological University
Block S1, Nanyang Avenue, Singapore 639798

Abstract–Analysis of frequency selective surface with gridded square element using accurate integral equation technique is considered in this paper. An improved subsectional current approximation model is proposed. Two more terms of basis function, the downward half triangle (DHT) term and the upward half triangle (UHT) term, besides the commonly adopted rooftop function, are included to expand the induced current. The additional terms are used to account for the effect of the induced currents at the corners of the outer square of the unit cell. Green's functions are derived by using spectral domain immittance approach and the incident fields are derived by using the z-directed potential. The computed results are in good agreement with the measured results.

1. **Introduction**
2. **Formulation**
3. **Subsectional Model for Current Approximation**
4. **Spectral Green's Function**
5. **Incident Fields**
6. **Numerical and Experimental Results**

7. Conclusions
References

1. INTRODUCTION

The technology of frequency selective surfaces (FSSs) [1–6] has a long
history of development. Over the past few decades, FSSs have found
numerous applications in both the commercial and military sectors
to provide multiple frequency band operation. An example in our
daily life is the screen door of a microwave oven. It consists of a
periodic array of metallic holes and is designed to reflect microwave
energies at 2.45 GHz while allowing light to pass through. Extensive
analytic research [6–17] has been performed to predict the reflection
and transmission properties of FSSs. The gridded square FSS [1, 5, 11]
is proposed to give closer reflection/transmission band ratios between
1.3 to 2.1 compared to > 2.5 for the single square FSS. Previously, it
has been analyzed with the equivalent circuit model (ECM) [5, 11]. But
the ECM cannot accurately model the effects caused by the dielectric
substrate and superstrate. The accurate integral equation technique
[1–4, 6, 10, 12, 14] with rooftop basis functions [18] has been used to
analyze many kinds of FSS embedded in dielectrics. It is observed
that the previous subsectional current approximation model assumes
that the induced current vanishes at the edges of the unit cell of FSSs.
However, the induced current does not vanish at the corners of the unit
cell for FSS with gridded square element. Therefore, the model has to
be modified.

   In this paper, an improved subsectional current approximation
model is proposed to analyze the frequency response of FSS with grid-
ded square element. Two more terms of basis function, the downward
half triangle (DHT) term and the upward half triangle (UHT) term,
besides the commonly adopted rooftop function, are included to ex-
pand the induced current. Accurate integral equation technique with
Galerkin's method is used to predict the reflection and transmission
properties. The predicted results are in good agreement with the mea-
sured results.

2. FORMULATION OF THE INTEGRAL EQUATIONS

The configuration of the multilayered FSS with gridded square ele-
ment is depicted in Fig. 1. There are M conducting screens within
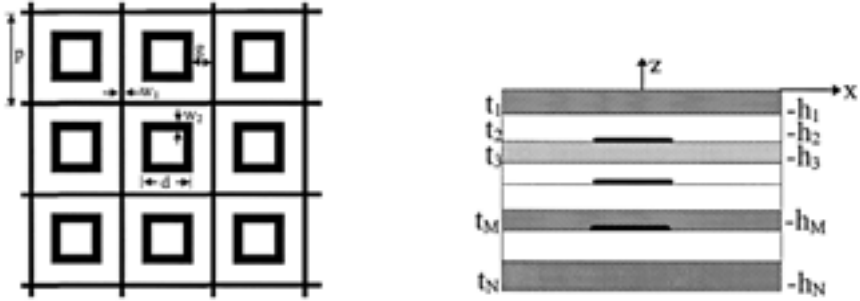
Figure 1. A multilayered FSS with gridded square element.

the N-layer stratified medium. ε_i, μ_i, t_i are the permittivity, permeability, and the thickness of the ith layer respectively. The incident field will induce currents on the conducting surfaces, which, in turn, radiate scattered fields. The induced currents on each of the conducting surfaces are related to the incident fields by the equation

$$\sum_{j=1}^{M} \sum_{m=-\infty}^{\infty} \sum_{n=-\infty}^{\infty} \begin{bmatrix} \widetilde{G}_{xx}^{l(i),l(j)}(\alpha_m, \beta_n) & \widetilde{G}_{xy}^{l(i),l(j)}(\alpha_m, \beta_n) \\ \widetilde{G}_{yx}^{l(i),l(j)}(\alpha_m, \beta_n) & \widetilde{G}_{yy}^{l(i),l(j)}(\alpha_m, \beta_n) \end{bmatrix}$$

$$\cdot \begin{bmatrix} \widetilde{J}_x^j(\alpha_m, \beta_n) \\ \widetilde{J}_y^j(\alpha_n, \beta_n) \end{bmatrix} e^{j\alpha_m x} e^{j\beta_n y} = - \begin{bmatrix} E_{x,l(i)}^{inc}(x,y) \\ E_{y,l(i)}^{inc}(x,y) \end{bmatrix} \quad i = 1, 2, \ldots, M \quad (1)$$

where $G_{xx}^{l(i),l(j)}(\alpha_m, \beta_n)$, $G_{xy}^{l(i),l(j)}(\alpha_m, \beta_n)$, $G_{yx}^{l(i),l(j)}(\alpha_m, \beta_n)$, and $G_{yy}^{l(i),l(j)}(\alpha_m, \beta_n)$ are the spectral Green's functions which will be derived shortly. The superscript $l(i)$ and $l(j)$ correspond to the layer number of the ith and jth conducting surface respectively. $E_{x,l(i)}^{inc}(x,y)$ and $E_{y,l(i)}^{inc}(x,y)$ are the incident electric field on the ith conducting surface in the presence of the dielectric structure but with all conducting patches removed.

$$\begin{bmatrix} E_{x,l(i)}^{inc}(x,y) \\ E_{y,l(i)}^{inc}(x,y) \end{bmatrix} = \begin{bmatrix} E_{x0,l(i)}^{inc} \\ E_{y0,l(i)}^{inc} \end{bmatrix} e^{jk_x^{inc}x} e^{jk_y^{inc}y}$$

$$\alpha_m = \frac{2m\pi}{a} + k_x^{inc} \qquad \beta_n = \frac{2n\pi}{b} + k_y^{inc}$$

$$k_x^{inc} = k_0 \sin\theta\cos\phi \qquad k_y^{inc} = k_0 \sin\theta\sin\phi \qquad k_0 = \omega\sqrt{\mu_0\varepsilon_0}$$

Expand the induced current in the form

$$J_x^j(x, y) = \sum_{i=1}^{M_1} I_{xi}^j B_{xi}(x, y) \tag{2}$$

$$J_y^j(x, y) = \sum_{i=1}^{N_1} I_{yi}^j B_{yi}(x, y) \tag{3}$$

where M_1 and N_1 are the total number of basis functions for the induced currents on each screen in x and y direction respectively, $B_{xi}(x, y)$ and $B_{yi}(x, y)$ are the ith basis function in x and y direction respectively.

One gets

$$-\begin{bmatrix} \mathbf{E}_{x0}^{inc} \\ \mathbf{E}_{y0}^{inc} \end{bmatrix} e^{jk_x^{inc}x} e^{jk_y^{inc}y} = \sum_{m=-\infty}^{\infty} \sum_{n=-\infty}^{\infty} \begin{bmatrix} \widetilde{\mathbf{G}}_{xx}(\alpha_m, \beta_n) & \widetilde{\mathbf{G}}_{xy}(\alpha_m, \beta_n) \\ \widetilde{\mathbf{G}}_{yx}(\alpha_m, \beta_n) & \widetilde{\mathbf{G}}_{yy}(\alpha_m, \beta_n) \end{bmatrix}$$

$$\cdot \begin{bmatrix} \widetilde{\mathbf{B}}_x(\alpha_m, \beta_n) & 0 \\ 0 & \widetilde{\mathbf{B}}_y(\alpha_m, \beta_n) \end{bmatrix} \cdot \begin{bmatrix} \mathbf{I}_x \\ \mathbf{I}_y \end{bmatrix} e^{j\alpha_m x} e^{j\beta_m y} \tag{4}$$

where

$$\mathbf{E}_{p0}^{inc} = \begin{bmatrix} E_{p0,l(1)}^{inc} & E_{p0,l(2)}^{inc} & \cdots & E_{p0,l(M)}^{inc} \end{bmatrix}^T$$

$$\widetilde{\mathbf{G}}_{pr} = \begin{bmatrix} \widetilde{G}_{pr}^{l(1),l(1)} & \widetilde{G}_{pr}^{l(1),l(2)} & \cdots & \widetilde{G}_{pr}^{l(1),l(M)} \\ \widetilde{G}_{pr}^{l(2),l(1)} & \widetilde{G}_{pr}^{l(2),l(2)} & \cdots & \widetilde{G}_{pr}^{l(2),l(M)} \\ \cdots & \cdots & \cdots & \cdots \\ \widetilde{G}_{pr}^{l(M),l(1)} & \widetilde{G}_{pr}^{l(M),l(2)} & \cdots & \widetilde{G}_{pr}^{l(M),l(M)} \end{bmatrix}$$

$$\mathbf{B}_p = \begin{bmatrix} \mathbf{B}_p^1 & & & \\ & \mathbf{B}_p^2 & & \\ & & \cdots & \\ & & & \mathbf{B}_p^M \end{bmatrix}$$

$$\widetilde{\mathbf{B}}_p^j(\alpha, \beta) = \begin{bmatrix} \widetilde{B}_{p1}^j(\alpha, \beta) & \cdots & \widetilde{B}_{pM_1}^j(\alpha, \beta) \end{bmatrix}$$

$$\mathbf{I}_p = \begin{bmatrix} \mathbf{I}_p^1 & \cdots & \mathbf{I}_p^M \end{bmatrix}^T \quad \mathbf{I}_p^j = \begin{bmatrix} I_{p1}^j & \cdots & I_{pM_1}^j \end{bmatrix} \quad p, r = x, y$$

the superscript T stands for matrix transpose.

Using Galerkin's method [19], one gets

$$
-\begin{bmatrix} \widetilde{\mathbf{T}}_x^+ \left(k_x^{inc}, k_y^{inc}\right) & 0 \\ 0 & \widetilde{\mathbf{T}}_x^+ \left(k_x^{inc}, k_y^{inc}\right) \end{bmatrix} \cdot \begin{bmatrix} \mathbf{E}_{x0}^{inc} \\ \mathbf{E}_{y0}^{inc} \end{bmatrix}
$$

$$
= \sum_{m=-\infty}^{\infty} \sum_{n=-\infty}^{\infty} \begin{bmatrix} \widetilde{\mathbf{T}}_x^+(\alpha_m, \beta_n) & 0 \\ 0 & \widetilde{\mathbf{T}}_x^+(\alpha_m, \beta_n) \end{bmatrix}
$$

$$
\cdot \begin{bmatrix} \widetilde{\mathbf{G}}_{xx}(\alpha_m, \beta_n) & \widetilde{\mathbf{G}}_{xy}(\alpha_m, \beta_n) \\ \widetilde{\mathbf{G}}_{yx}(\alpha_m, \beta_n) & \widetilde{\mathbf{G}}_{yy}(\alpha_m, \beta_n) \end{bmatrix}
$$

$$
\cdot \begin{bmatrix} \widetilde{\mathbf{B}}_x(\alpha_m, \beta_n) & 0 \\ 0 & \widetilde{\mathbf{B}}_y(\alpha_m, \beta_n) \end{bmatrix} \cdot \begin{bmatrix} \mathbf{I}_x \\ \mathbf{I}_y \end{bmatrix} \tag{5}
$$

where

$$
\mathbf{T}_p = \begin{bmatrix} \mathbf{T}_p^1 & & & \\ & \mathbf{T}_p^2 & & \\ & & \cdots & \\ & & & \mathbf{T}_p^M \end{bmatrix}
$$

$$
\widetilde{\mathbf{T}}_p^j(\alpha, \beta) = \begin{bmatrix} \widetilde{T}_{p1}^j(\alpha, \beta) & \cdots & \widetilde{T}_{pM_1}^j(\alpha, \beta) \end{bmatrix}
$$

the superscript $+$ stands for matrix conjugate transpose.

Eq. (5) can be solved to determine the unknown expansion coefficients of the induced current by either direct matrix method or other iterative method such as conjugate gradient method. After determining the induced current, the reflection and transmission coefficients for each of the Floquet modes can be expressed as

$$
R_{mn}^{TE} = \frac{j \left\{ \beta_n \left[\widetilde{E}_{x,0}^s(\alpha_m, \beta_n) + \widetilde{E}_x^r \delta_{mn} \right] - \alpha_m \left[\widetilde{E}_{y,0}^s(\alpha_m, \beta_n) + \widetilde{E}_y^r \delta_{mn} \right] \right\}}{\alpha_m^2 + \beta_n^2}
$$

$$
\tag{6}
$$

$$
R_{mn}^{TM} = \frac{-\left\{ \alpha_m \left[\widetilde{E}_{x,0}^s(\alpha_m, \beta_n) + \widetilde{E}_x^r \delta_{mn} \right] + \beta_n \left[\widetilde{E}_{y,0}^s(\alpha_m, \beta_n) + \widetilde{E}_y^r \delta_{mn} \right] \right\}}{(\alpha_m^2 + \beta_n^2) \gamma_{mn}/\omega \varepsilon_0}
$$

$$
\tag{7}
$$

$$
T_{mn}^{TE} = \frac{j \left\{ \beta_n \left[\widetilde{E}_{x,N}^s(\alpha_m, \beta_n) + \widetilde{E}_x^t \delta_{mn} \right] - \alpha_m \left[\widetilde{E}_{y,N}^s(\alpha_m, \beta_n) + \widetilde{E}_y^t \delta_{mn} \right] \right\}}{\alpha_m^2 + \beta_n^2}
$$

$$
\cdot e^{\gamma_{mn} h_N} \tag{8}
$$

$$T_{mn}^{TM} = \frac{\left\{ \alpha_m \left[\widetilde{E}_{x,N}^s(\alpha_m, \beta_n) + \widetilde{E}_x^t \delta_{mn} \right] + \beta_n \left[\widetilde{E}_{y,N}^s(\alpha_m, \beta_n) + \widetilde{E}_y^t \delta_{mn} \right] \right\}}{\left(\alpha_m^2 + \beta_n^2 \right) \gamma_{mn}/\omega\varepsilon_0}$$

$$\cdot\, e^{\gamma_{mn} h_N} \tag{9}$$

where

$$\begin{bmatrix} \widetilde{E}_{x,i}^s \\ \widetilde{E}_{y,i}^s \end{bmatrix} = \sum_{j=1}^{M} \begin{bmatrix} \widetilde{G}_{xx}^{i,l(j)}(\alpha_m, \beta_n) & \widetilde{G}_{xy}^{i,l(j)}(\alpha_m, \beta_n) \\ \widetilde{G}_{yx}^{i,l(j)}(\alpha_m, \beta_n) & \widetilde{G}_{yy}^{i,l(j)}(\alpha_m, \beta_n) \end{bmatrix} \cdot \begin{bmatrix} \widetilde{J}_x^j(\alpha_m, \beta_n) \\ \widetilde{J}_y^j(\alpha_n, \beta_n) \end{bmatrix} \quad i = 0, N$$

$$\gamma_{mn} = \sqrt{\alpha_m^2 + \beta_n^2 - k_0^2}$$

$\widetilde{E}_P^r$ and $\widetilde{E}_P^t$ are the spectral domain electric field reflected at $z = 0^+$ and transmitted at $z = h_N^-$ respectively in the presence of the dielectric structure but with all conducting patches removed.

3. SUBSECTIONAL MODEL FOR CURRENT APPROXIMATION

Rooftop basis function has been chosen to approximate the distribution of the induced current on FSS screens, i.e.,

$$B_{xi}(x, y) = R_{xpq}(x, y) \tag{10}$$
$$B_{yi}(x, y) = R_{ypq}(x, y) \tag{11}$$

where

$$R_{xpq}(x, y) = R_x(x - p\Delta x, y - q\Delta y) \quad p = 1, N_x \quad q = 0, N_y$$
$$R_{ypq}(x, y) = R_y(x - p\Delta x, y - q\Delta y) \quad p = 0, N_x \quad q = 1, N_y$$
$$R_x(x, y) = \Lambda_x(x)\Pi_x(y) \qquad R_y(x, y) = \Pi_y(x)\Lambda_y(y)$$
$$\Lambda_x(x) = \begin{cases} 1 - |x|/\Delta x & |x| \le \Delta x \\ 0 & \text{elsewhere} \end{cases} \quad \Pi_x(y) = \begin{cases} 1 & 0 \le y \le \Delta y \\ 0 & \text{elsewhere} \end{cases}$$
$$\Pi_y(x) = \begin{cases} 1 & 0 \le x \le \Delta x \\ 0 & \text{elsewhere} \end{cases} \qquad \Lambda_y(y) = \begin{cases} 1 - |y|/\Delta y & |y| \le \Delta y \\ 0 & \text{elsewhere} \end{cases}$$
$$\Delta x = a/(N_x + 1) \qquad\qquad \Delta y = b/(N_y + 1)$$

N_x and N_y are the total number of subsections for the unit cell in x and y direction respectively.

It is observed that the above model assumes that the induced current vanishes at the edges of the unit cell of FSSs. However, the induced

current does not vanish at the corners of the unit cell for FSS with gridded square element. Therefore, the above model has to be modified to account for the induced at the corners.

Two more terms, the downward half triangle (DHT) term and the upward half triangle (UHT) term, are included to expand the induced current for FSS with gridded square element

$$J_x^j(x, y) = \sum_{i=1}^{M_1} I_{xi}^j B_{xi}(x, y) + \sum_{i=0}^{M_2-1} I_{xi}^{DHT,j} DHT_{xi}(x, y)$$

$$+ \sum_{i=0}^{M_2-1} I_{xi}^{UHT,j} UHT_{xi}(x, y) \tag{12}$$

$$J_y^j(x, y) = \sum_{i=1}^{M_1} I_{yi}^j B_{xi}(x, y) + \sum_{i=0}^{M_2-1} I_{yi}^{DHT,j} DHT_{yi}(x, y)$$

$$+ \sum_{i=0}^{M_2-1} I_{yi}^{UHT,j} UHT_{yi}(x, y) \tag{13}$$

where

$$DHT_{xi}(x, y) = W_x(x)\Delta_x(x)\Pi_x(y - i\Delta y)$$
$$DHT_{yi}(x, y) = \Pi_y(x - i\Delta x)W_y(y)\Lambda_y(y)$$
$$UHT_{xi}(x, y) = W_x(x - N_x\Delta x)\Lambda_x[x - (N_x + 1)\Delta x]\Pi_x(y - i\Delta y)$$
$$UHT_{yi}(x, y) = \Pi_y(x - i\Delta x)W_y(y - N_y\Delta y)\Lambda_y[y - (N_y + 1)\Delta y]$$
$$W_x(x) = \begin{cases} 1 & 0 \leq x \leq \Delta x \\ 0 & \text{elsewhere} \end{cases} \qquad W_y(y) = \begin{cases} 1 & 0 \leq y \leq \Delta y \\ 0 & \text{elsewhere} \end{cases}$$

M_2 is the total number of DHT/UHT terms which depends on the width of the gridded square W_1.

The downward half triangle terms in Eqs. (12) and (13) are used to represent the corner current at the left/bottom corner of the unit cell, while the upward half triangle terms are used to represent the corner current at the right/top corner of the unit cell.

According to the Floquet's theorem [20] for periodic structures, the following condition must be imposed

$$I_{xi}^{UHT,j} = e^{jk_x^{inc}p} I_{xi}^{DHT,j} \tag{14}$$

$$I_{yi}^{UHT,j} = e^{jk_y^{inc}p} I_{yi}^{DHT,j} \tag{15}$$
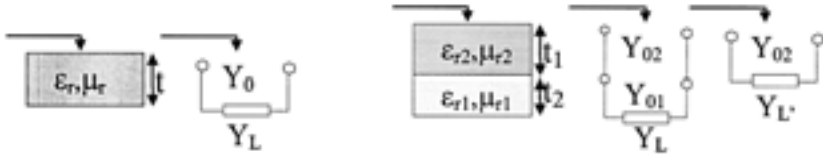
Figure 2. Equivalent transmission line model.

The basis function matrix and test function matrix in Eq. (5) should be modified accordingly.

4. SPECTRAL GREEN'S FUNCTION

In this section, the spectral Green's functions in Eq. (1) relating the current on the screen at the jth interface (between the jth and $(j+1)$th layer) and the scattered field at the ith interface are derived.

By the spectral-domain immittance approach [21, 22], one gets

$$
\begin{bmatrix} \widetilde{G}_{xx}^{ij}(\alpha,\beta) & \widetilde{G}_{xy}^{ij}(\alpha,\beta) \\ \widetilde{G}_{yx}^{ij}(\alpha,\beta) & \widetilde{G}_{yy}^{ij}(\alpha,\beta) \end{bmatrix}
$$
$$
= \begin{bmatrix} \widetilde{Z}^{TE,ij}\sin^2\theta + \widetilde{Z}^{TM,ij}\cos^2\theta & \left(\widetilde{Z}^{TM,ij} - \widetilde{Z}^{TE,ij}\right)\cos\theta\sin\theta \\ \left(\widetilde{Z}^{TM,ij} - \widetilde{Z}^{TE,ij}\right)\cos\theta\sin\theta & \widetilde{Z}^{TM,ij}\sin^2\theta + \widetilde{Z}^{TE,ij}\cos^2\theta \end{bmatrix} \quad (16)
$$

where
$$
\cos\theta = \alpha/\sqrt{\alpha^2 + \beta^2} \qquad \sin\theta = \beta/\sqrt{\alpha^2 + \beta^2}
$$

Therefore, to derive the Green's function, one needs to derive Z in Eq. (16). Consider the situation depicted in Fig. 2 and its transmission line equivalent model. According to the theory of transmission lines [23], the input admittance looking downward for case (a) is

$$
Y_{in} = Y_0 \frac{Y_0 + Y_L \coth\gamma t}{Y_0 \coth\gamma t + Y_L} \quad (17)
$$

where

$$
\gamma = \sqrt{\alpha^2 + \beta^2 - \varepsilon_r \mu_r k_0^2}
$$

By successively using of Eq. (17), the input admittance looking downward for case (b) is obtained

$$
Y_{in} = Y_{02} \frac{Y_{02} + Y_{L'} \coth\gamma_2 t_2}{Y_{02} \coth\gamma_2 t_2 + Y_{L'}} \quad (18)
$$
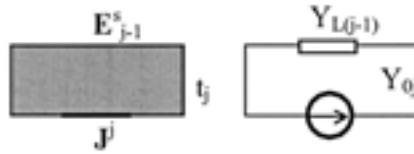
Figure 3. Relation between the current and the scattered field at different location.

where

$$Y_{L'} = Y_{01} \frac{Y_{01} + Y_L \coth \gamma_1 t_1}{Y_{01} \coth \gamma_1 t_1 + Y_L} \tag{19}$$

$$\gamma_i = \sqrt{\alpha^2 + \beta^2 - \varepsilon_{ri}\mu_{ri}k_0^2}$$

The TE and TM case characteristic admittance of a medium are defined as follows

$$Y_0^{TE} = -\gamma/j\omega\mu \qquad Y_0^{TM} = -j\omega\varepsilon/\gamma$$

The input admittance looking upward can similarly be obtained.

Therefore, the input impedance that relates the current on the screen at the jth interface and the scattered field at the same interface due to this current is then

$$Z^{TM/TE,jj} = 1 \Big/ \left(Y_{bottom}^{e/h} + Y_{top}^{e/h}\right) \tag{20}$$

where Y_{bottom} and Y_{top} represent the input admittance looking downward and upward from the jth interface respectively. The superscript e corresponds to the TM case, and the superscript h corresponds to the TE case.

On the other hand, when the scattered field is evaluated at a distance t away from the current source as depicted in Fig. 3, one needs to modify Eq. (20) to obtain the impedance $Z^{TM/TE,(j-1)j}$. In Fig. 3, $Y_{L(j-1)}$ is the input admittance looking upward from the top surface, that is, it includes all layers above the $(j-1)$th interface. It is obtained by successively using Eq. (18). To transfer the impedance to that at the $(j-1)$th interface, one needs to multiply Eq. (20) by the factor

$$Y_{tran}^{(j-1),j} = Y_{0,j} \Big/ \left(Y_{0j} \cosh \gamma_j t_j + Y_{L(j-1)} \sinh \gamma_j t_j\right) \tag{21}$$

Therefore

$$Z^{TM/TE,(j-1)j} = Y_{tran}^{e/h,(j-1)j} Z^{TM/TE,jj} \tag{22}$$
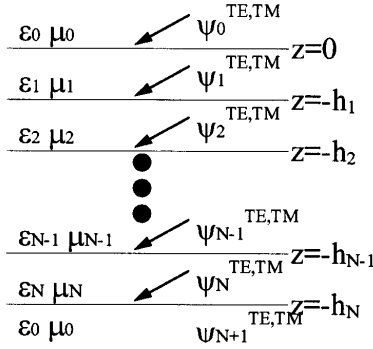
Figure 4. Incident fields.

By successively using Eq. (22), one obtains the impedance $Z^{TM/TE,ij}$ as

$$
Z^{TM/TE,ij} = Z^{TM/TE,jj} \cdot \begin{cases} \displaystyle\prod_{l=i+1}^{j} Y_{tran}^{e/h,(l-1)l} & i < j \\ \displaystyle\prod_{l=j}^{i-1} Y_{tran}^{e/h,(l-1)l} & i > j \end{cases} \tag{23}
$$

Substituting Eq. (23) into Eq. (16), one finally obtains the spectral Green's functions relating the current on the screen at the jth interface and the scattered field at the ith interface.

5. INCIDENT FIELDS

The incident fields for TE and TM polarizations can be derived by using the z-directed potential ψ. The incident field is calculated in the presence of the dielectric structures but with all conducting patches removed. A general configuration is depicted in Fig. 4. The potential of each region is defined as follows:

$$
\psi_0^{TM,TE} = e^{j\alpha_0 x} e^{j\beta_0 y} e^{\gamma_0 z} + \mathrm{Re}^{j\alpha_0 x} e^{j\beta_0 y} e^{-\gamma_0 z} \tag{24}
$$

$$
\psi_1^{TM,TE} = e^{j\alpha_0 x} e^{j\beta_0 y} \left(C_{11} e^{\gamma_1 z} + C_{12} e^{-\gamma_1 z} \right) \tag{25}
$$

$$
\vdots
$$

$$
\psi_N^{TM,TE} = e^{j\alpha_0 x} e^{j\beta_0 y} \left(C_{N1} e^{\gamma_N z} + C_{N2} e^{-\gamma_N z} \right) \tag{26}
$$

$$
\psi_{N+1}^{TM,TE} = T e^{j\alpha_0 x} e^{j\beta_0 y} e^{\gamma_0 z} \tag{27}
$$

where

$$\alpha_0 = k_x^{inc} \qquad \beta_0 = k_y^{inc} \qquad \gamma_0 = \sqrt{\alpha_0^2 + \beta_0^2 - k_0^2} = jk_0 \cos\theta$$

To enforce the continuity of the tangential electric and magnetic fields at the dielectric interfaces, we use the following equations:

TE case

$$E_x = -\frac{\partial\psi^{TE}}{\partial y} \qquad E_y = \frac{\partial\psi^{TE}}{\partial x} \qquad (28)$$

$$H_x = \frac{1}{j\omega\mu}\frac{\partial^2\psi^{TE}}{\partial x\partial z} \qquad H_y = \frac{1}{j\omega\mu}\frac{\partial^2\psi^{TE}}{\partial y\partial z} \qquad (29)$$

TM case

$$H_x = -\frac{\partial\psi^{TM}}{\partial y} \qquad H_y = \frac{\partial\psi^{TM}}{\partial x} \qquad (30)$$

$$E_x = \frac{1}{j\omega\varepsilon}\frac{\partial^2\psi^{TM}}{\partial x\partial z} \qquad E_y = \frac{1}{j\omega\varepsilon}\frac{\partial^2\psi^{TM}}{\partial y\partial z} \qquad (31)$$

The following equations are obtained

$$1 + R = C_{11} + C_{12} \qquad (32)$$

$$\gamma_0(1 - R) = \frac{\gamma_1}{\xi_{r1}}(C_{11} - C_{12}) \qquad (33)$$

$$\vdots$$

$$C_{i1}e^{-\gamma_i h_i} + C_{i2}e^{\gamma_i h_i} = C_{i+1,1}e^{-\gamma_{i+1}h_i} + C_{i+1,2}e^{\gamma_{i+1}h_i} \qquad (34)$$

$$\frac{\gamma_i}{\xi_{ri}}\left(C_{i1}e^{-\gamma_i h_i} - C_{i2}e^{\gamma_i h_i}\right) = \frac{\gamma_{i+1}}{\xi_{ri+1}}\left(C_{i+1,1}e^{-\gamma_{i+1}h_i} - C_{i+1,2}e^{\gamma_{i+1}h_i}\right)$$

$$i = 1, 2, \ldots, N - 1 \qquad (35)$$

$$\vdots$$

$$C_{N1}e^{-\gamma_N h_N} + C_{N2}e^{\gamma_N h_N} = Te^{-\gamma_0 h_N} \qquad (36)$$

$$\frac{\gamma_N}{\xi_{rN}}\left(C_{N1}e^{-\gamma_N h_N} - C_{N2}e^{\gamma_N h_N}\right) = T\gamma_0 e^{-\gamma_0 h_N} \qquad (37)$$

where $\xi_r = \mu_r$ and $\xi_r = \varepsilon_r$ for TE and TM incidence respectively.

In matrix form, it is

$$\mathbf{A} \cdot \mathbf{x} = \mathbf{b} \qquad (38)$$

where

$$\mathbf{x} = \begin{bmatrix} R & C_{11} & C_{12} & \cdots & C_{N1} & C_{N2} & T \end{bmatrix}^T$$
$$b = \begin{bmatrix} -1 & -\gamma_0 & 0 & \cdots & 0 & 0 & 0 \end{bmatrix}^T$$

$$A_{11} = 1 \qquad A_{12} = -1 \qquad A_{13} = -1$$
$$A_{21} = -\gamma_0 \qquad A_{22} = -\gamma_1/\xi_{r1} \qquad A_{23} = \gamma_1/\xi_{r1}$$

$$A_{2i+1,2i} = e^{-\gamma_i h_i} \qquad\qquad A_{2i+1,2i+1} = e^{\gamma_i h_i}$$
$$A_{2i+1,2i+2} = -e^{-\gamma_{i+1} h_i} \qquad\qquad A_{2i+1,2i+3} = e^{\gamma_{i+1} h_i}$$
$$A_{2i+2,2i} = \frac{\gamma_i}{\xi_{ri}} e^{-\gamma_i h_i} \qquad\qquad A_{2i+2,2i+1} = -\frac{\gamma_i}{\xi_{ri}} e^{\gamma_i h_i}$$
$$A_{2i+2,2i+2} = -\frac{\gamma_{i+1}}{\xi_{ri+1}} e^{-\gamma_{i+1} h_i} \qquad A_{2i+2,2i+3} = \frac{\gamma_{i+1}}{\xi_{ri+1}} e^{\gamma_{i+1} h_i}$$
$$i = 1, 2, \ldots, N-1$$

$$A_{2N+1,2N} = e^{-\gamma_N h_N} \qquad A_{2N+1,2N+1} = e^{\gamma_N h_N}$$
$$A_{2N+1,2N+2} = -e^{-\gamma_0 h_N} \qquad A_{2N+2,2N} = \frac{\gamma_N}{\xi_{rN}} e^{-\gamma_N h_N}$$
$$A_{2N+2,2N+1} = -\frac{\gamma_N}{\xi_{rN}} e^{\gamma_N h_N}$$
$$A_{2i+2,2i+2} = -\gamma_0 e^{-\gamma_0 h_N}$$

Eq. (38) is solved numerically to determine the values of all the coefficients in Eqs. (24)–(27). The incident field is subsequently obtained.

6. NUMERICAL AND EXPERIMENTAL RESULTS

In this section, we present some numerical results and compare them with the measured results.

Two single screen FSS with gridded square element printed on a 0.021 mm Mylar substrate with relative permittivity of about 3.0 is designed, analyzed and measured. The parameters of the FSS are shown in Table 1. The predicted and measured resonance frequencies are shown in Table 2 and the frequency response is shown in Fig. 5 and Fig. 6.

For comparison, the previous model is also applied to predict the frequency response of the above FSSs. The resonance frequencies are shown in Table 2 and the frequency response for $(45°, 1°)$ incidence is shown in Fig. 7 and Fig. 8. It is observed that the transmission resonance frequencies are unable to be predicted by the previous model.

Table 1. Dimension parameters of designed FSSs.

No.		p (mm)	w_1 (mm)	d (mm)	w_2 (mm)	g (mm)
1	Designed	4.0	0.4	2.4	0.2	0.6
	Manufactured	4.0	0.38	2.5	0.2	0.56
2	Designed	5.0	0.2	4.0	0.2	0.4
	Manufactured	5.04	0.18	4.1	0.22	0.38
3	-	6.8	0.425	5.525	0.85	0.425
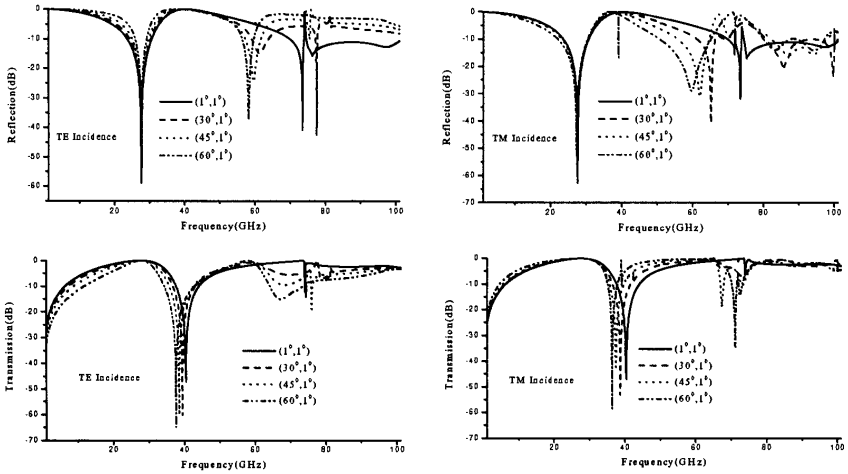
Figure 5. Frequency response of FFS #1.
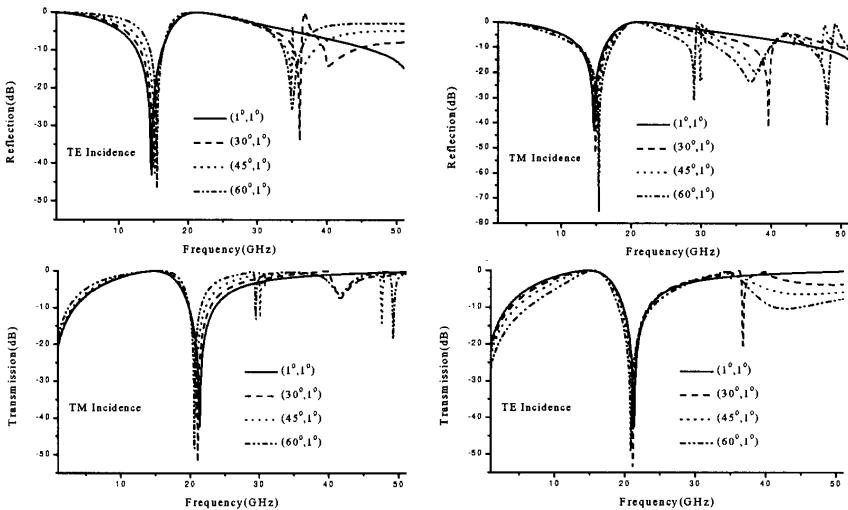
Figure 6. Frequency response of FFS #2.

Table 2. Predicted and measured resonance frequencies of FSSs in Table 1.

No.	Tansmission Frequency (GHz)				Refelection Frequency (GHz)			
	Ours	Previous	Measured	ECM	Ours	Previous	Measured	ECM
1	27.6	missed	26.8	27.0	40.4	40.7	40.4	39.1
2	14.7	missed	13.4	13.4	21.4	21.3	20.8	20.4
3	7.9	missed	-	-	14.8	15.0	-	-
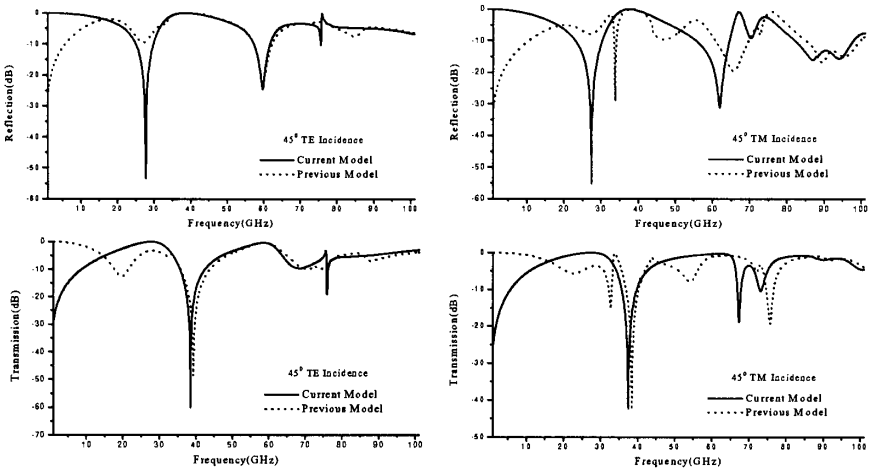
Figure 7. Frequency response of FFS #1 predicted by previous model.
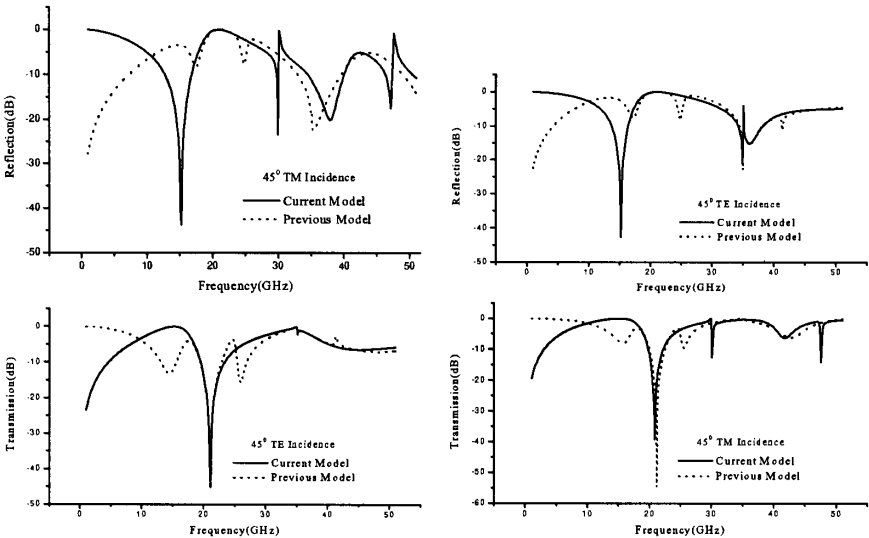
Figure 8. Frequency response of FFS #2 predicted by previous model.
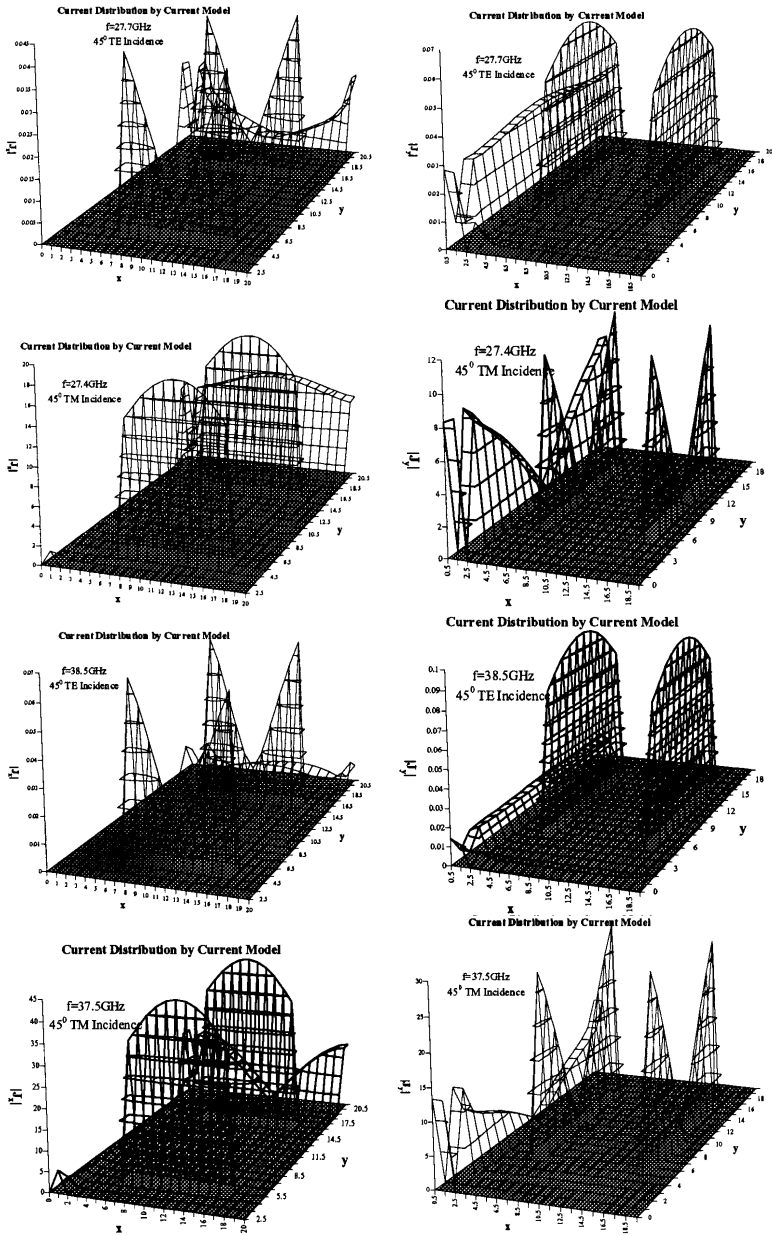
Figure 9. Current distribution over unit cell of FSS #1.
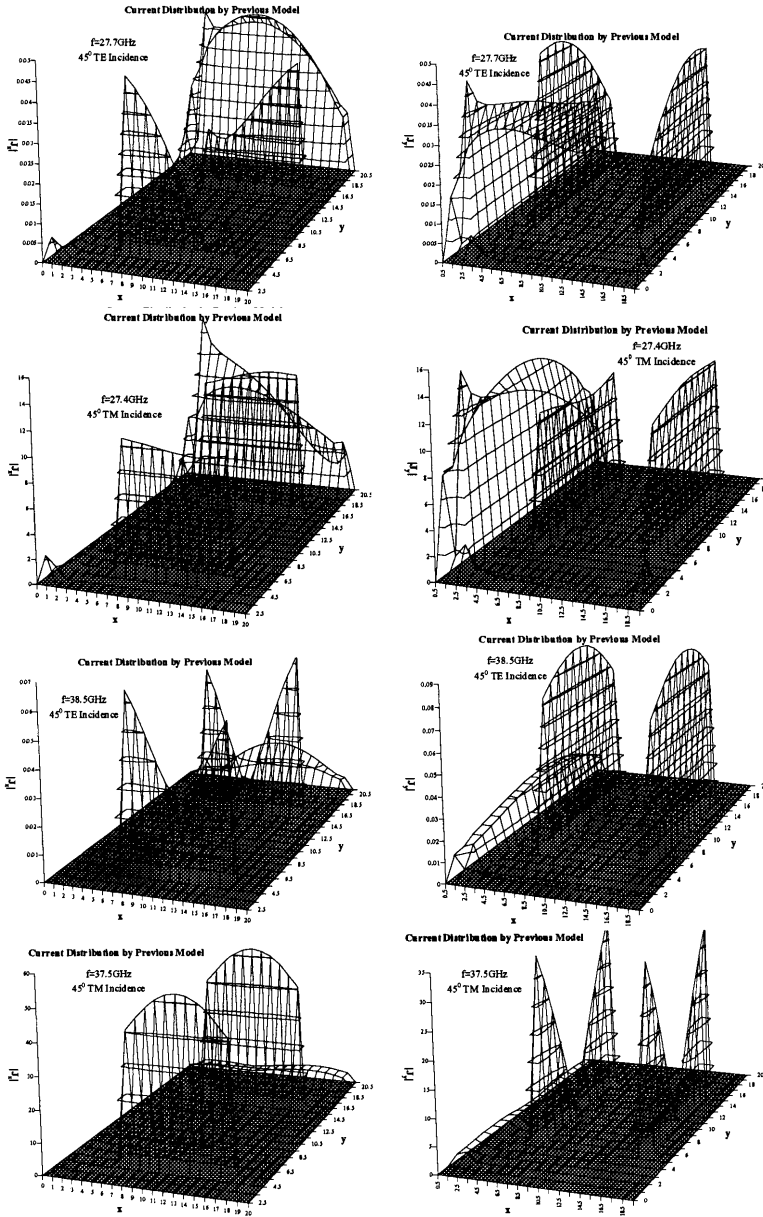
Figure 10. Current distribution over unit cell of FSS #1 by previous model.
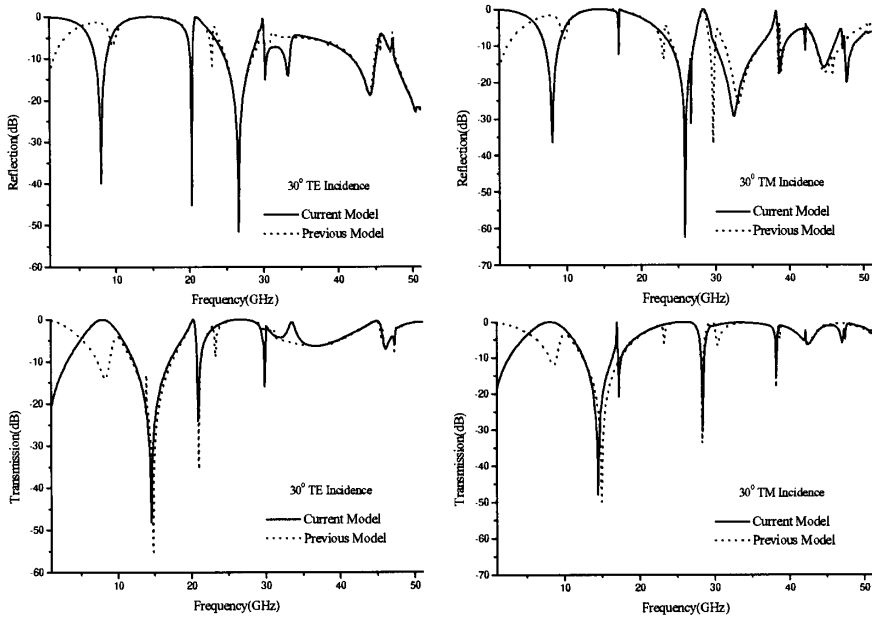
Figure 11. Frequency response of FSS #5.

The distribution of induced current over the unit cell of FSS #1 at resonance frequencies is depicted in Fig. 9. The distribution obtained using the previous model is shown in Fig. 10. It can be seen that great discrepancy exists between them which results in the difference of the predicted frequency response. The third example is one FSS embedded in dielectric medium with dielectric constant 2.2. Both the superstrate and substrate are 0.889 mm thick. The dimension parameters and the predicted resonance frequencies are also shown in Table 1 and 2 respectively. The frequency response for $(30°, 1°)$ incidence is shown in Fig. 11.

7. CONCLUSIONS

In this paper, An improved subsectional current approximation model is proposed to analyze FSS with gridded square element by accurate integral equation technique. Two more terms of basis function, the downward half triangle (DHT) term and the upward half triangle (UHT) term, besides the commonly adopted rooftop function, are included to expand the induced current. Green's functions are derived by

using spectral domain immittance approach and the incident fields are derived by using the z-directed potential. Numerical and experimental results are presented. Good agreement between the predicted and measured results is obtained.

REFERENCES

1. Wu, T. K., (Ed.), *Frequency Selective Surface and Grid Array,* Wiley, New York, 1995.

2. Vardaxoglou, J. C., *Frequency Selective Surfaces: Analysis and Design,* Wiley, New York, 1997

3. Tsao, C. H., "Spectral-domain approach for analyzing scattering from frequency selective surface," Ph.D. dissertation, University of Illinois at Urbana-Champaign, 1981.

4. Chan, C. H., "Investigation of iterative and spectral Galerkin techniques for solving electromagnetic boundary value problems," Ph.D. dissertation, University of Illinois at Urbana-Champaign, 1987.

5. Lee, C. K., "Modeling and design of frequency selective surfaces for reflector antennas," Ph.D. dissertation, Kent University, 1987.

6. Mittra, R., C. H. Chan, and T. Cwik, "Techniques for analyzing frequency selective surfaces-a review," *Proc. IEEE,* Vol. 76, No. 12, 1593–1615, 1988.

7. Chen, C. C., "Transmission through a conducting screen perforated periodically with apertures," *IEEE Trans. Microwave Theory Tech.,* Vol. MTT-18, No. 9, 627–632, 1970.

8. Lee, S. W., "Scattering by dielectric-loaded screen," *IEEE Trans. Antennas Propagat.,* Vol. AP-19, No. 5, 656–665, 1971.

9. Luebbers, R. J. and B. A. Munk, "Some effects of dielectric loading on periodic slot arrays," *IEEE Trans. Antennas Propagat.,* Vol. AP-26, No. 4, 536–542, 1978.

10. Rubin, B. J. and H. L. Bertoni, "Reflection from a periodically perforated plane using a subsectional current approximation," *IEEE Trans. Antennas Propagat.,* Vol. AP-31, No. 6, 829–836, 1983.

11. Lee, C. K., and R. J. Langley, "Equivalent circuit models for frequency selective surfaces at oblique angle of incidence," *IEE Proc. Microwaves, Antennas, Propagat.,* Vol. 132, No. 6, 395–398, 1985.

12. Cwik, T. A. and R. Mittra, "Scattering from a periodic array of free-standing arbitrarily shaped perfectly conducting or resistive patches," *IEEE Trans. Antennas Propagat.,* Vol. AP-35, No. 11, 1226–1234, 1987.

13. Cwik, T. and R. Mittra, "The cascade connection of planar periodic surfaces and lossy dielectric layers to form an arbitrary periodic screen," *IEEE Trans. Antennas Propagat.,* Vol. AP-35, No. 12, 1397–1405, 1987.

14. Chan, C. H., and R. Mittra, "On the analysis of frequency-selective surfaces using subdomain basis functions," *IEEE Trans. Antennas Propagat.,* Vol. AP-38, No. 1, 40–50, 1990.

15. Styllanou, A., P. Debono, and J. C. Vardaxoglou, "Iterative computation of current and field distributions in multilayer frequency selective surfaces," *IEE Proc. Microwaves, Antennas, Propagat.,* Vol. 139, No. 6, 535–541, 1992.

16. Prescott, D. T., and N. V. Shuley, "A technique for analyzing frequency selective surfaces using the finite-difference time-domain method," *1994 IEEE Int. Antennas Propagat. Symp. Dig.,* 2152–2155, 1994.

17. Roden, J. A., et al., "Time-domain analysis of periodic structures at oblique incidence: orthogonal and nonorthogonal FDTD implementations," *IEEE Trans. Microwave Theory Tech.,* Vol. MTT-46, No. 4, 420–427, 1998.

18. Glisson, A. W., and D. R. Wilton, "Simple and efficient numerical methods for problems of electromagnetic radiation and scattering from surfaces," *IEEE Trans. Antennas Propagat.,* Vol. AP-28, No. 5, 593–603, 1980.

19. Harrington, R. F., *Field Computation by Moment Methods,* IEEE Press, New York, 1993.

20. Ishimaru, A., *Electromagnetic Wave Propagation, Radiation, and Scattering,* Prentice-Hall, Englewood Cliffs, NJ, 1991.

21. Itoh, T., "Spectral domain immittance approach for dispersion characteristics of generalized printed transmission lines," *IEEE Trans. Microwave Theory Tech.,* Vol. MTT-28, No. 7, 733–736, 1980.

22. Das, N. K., and D. M. Pozar, "A generalized spectral-domain Green's function for multilayer dielectric substrate with application to multilayer transmission lines," *IEEE Trans. Microwave Theory Tech.,* Vol. MTT-35, No. 3, 326–335, 1987.

23. Cheng, D. K., *Field and Wave Electromagnetics,* Addison-Wesley, 1983.